Energy Conversion and Management 307 (2024) 118376

Contents lists available at ScienceDirect

Energy Conversion and Management

journal homepage: www.elsevier.com/locate/enconman

Techno-economic analysis, emergy assessment, and optimization using response surface methodology of a solar and biomass-based co-generation system

Soheil Khosravi [a], Dibyendu Roy [b], Rahim Khoshbakhti Saray [c], Elaheh Neshat [c], Ahmad Arabkoohsar [a,*]

[a] Department of Civil and Mechanical Engineering, Technical University of Denmark, Kgs. Lyngby, Denmark
[b] Department of Engineering, Durham University, Durham DH1 3LE, UK
[c] Faculty of Mechanical Engineering, Sahand University of Technology, Tabriz, Iran

A R T I C L E I N F O

Keywords:
Gasification
CO_2 capture
Sustainability
Renewable energy
Response Surface Methodology
Solar energy
Calcium lopping

A B S T R A C T

Integrating renewable energy sources into systems is crucial for sustainability and reducing CO_2 emissions. The sorption-enhanced gasification process, when combined with renewables, offers a path toward sustainable energy systems. In this study, a novel integration of a solar-based sorption-enhanced gasification process for biomass is proposed, aiming for electricity and hydrogen generation. The entire system's performance has been investigated from the perspectives of energy, exergy, economics, and emergy analysis.

Furthermore, response surface methodology is employed to optimize the overall system performance in terms of energy and exergy efficiencies and the levelized cost of energy. The study's results reveal that the integrated system shows its optimum operational condition at a steam-to-biomass ratio of 0.53 and a CO_2 capture efficiency of 65 %. The optimum energy efficiency of the overall system is determined to be 67.2 % with a net electrical power generation of 5.251 MW. The optimum exergy efficiency for the whole system is determined at 71.89 %. Optimization results report a levelized cost of energy of 7.87 \$/MWh. From a sustainability analysis perspective, emergy analysis results indicate that the introduced system, with a renewability index of 0.22, has a low dependency on non-renewable inputs. With a sustainability index of 1.95, the system qualifies as moderately sustainable, demonstrating superior performance compared to conventional co-generation systems.

1. Introduction

The growth of the population and the progress of industrialization contribute to an increased demand for energy [1]. Approximately 70 % of the global energy demand is met by the utilization of fossil fuels, resulting in the release of greenhouse gases, notably carbon dioxide (CO_2), which contributes significantly to the phenomenon of global warming [2]. To effectively mitigate the emissions of greenhouse gases, with a particular focus on CO_2, it is imperative to consider a range of strategic actions. These include the substitution of outdated and ineffective plants with the adoption of advanced energy-efficient technologies, the expansion of renewable energy sources, and the utilization of carbon capture and storage (CCS) technologies [3]. These actions can be successful in meeting the targets established by the Intergovernmental Panel on Climate Change (IPCC) to keep global warming below 2 °C [4].

Sorption-enhanced gasification (SEG) is an innovative approach for increasing the hydrogen (H_2) concentration in syngas. SEG systems, equipped with CO_2 removal, offer promise for cleaner energy production from biomass while also reducing greenhouse gas emissions. The SEG system mainly integrates biomass gasification and CO_2 capture processes. Its adaptability allows easy integration with waste heat recovery cycles [5]; consequently, various studies have explored each of these subprocesses. Dziva et al. [6] proposed a novel two-staged SEG system, which includes an autothermal moving bed reformer and a calcium looping (CaL) process. They optimized it according to the CaL ratio, steam-to-carbon ratio, and feed temperatures of the moving bed reformer. Under optimal conditions, the proposed system can produce 99 % H_2 and achieve an overall efficiency of 58.7 %. In another similar study, Dziva et al. [7] conducted a kinetic analysis for a H_2 production system through a SEG process. Through the utilization of a moving bed reformer, the complete conversion of all tars was achieved, resulting in a

* Corresponding author.
E-mail address: ahmar@dtu.dk (A. Arabkoohsar).

https://doi.org/10.1016/j.enconman.2024.118376
Received 31 January 2024; Received in revised form 5 March 2024; Accepted 27 March 2024
Available online 3 April 2024

Nomenclature

BL	Lifetime (years)
C	Cost rate ($/h)
Calc	Calciner
CaL	Calcium Looping
CE	CO_2 Capture Efficiency (%)
CYC	Cyclone
EIR	Emergy Investment Ratio
ELR	Environmental Load Ratio
ESI	Emergy Sustainable Index
Ex	Exergy
F	Economic Emergy Inputs
F_0	Flow rate of fresh limestone (kmol/s)
F_{CO2}	CO_2 Molar fraction in the gas feed
FW	Feed Water Heater
G	Gasifier
HX	Heat Exchanger
HRSG	Heat Recovery Steam Generator
HPT	High-Pressure Turbine
LCOE	Levelized Cost of Energy
LHV	Lower Heating Value
LPT	Low-Pressure Turbine
MC	Moisture Content (%)
MSW	Municipal Solid Waste
N	Non-Renewable Local Source
PSA	Pressure Swing Adsorption
R	Renewable Local Source
RMS	Root-Mean-Square
RSM	Response Surface Methodology
SB	Steam to Biomass Ratio
SEG	Sorption Enhanced Gasification
Y	Total Emergy Yield (Sej/year)
T	Temperature
%R	Renewability Index

Greek Symbols

η	Efficiency
ω	Moisture/Dry Ash-Free MSW Ratio
ε	Steam to the Dry Ash-Free MSW Ratio

Subscripts

abs	Absorbed
ave	Average
ch	Chemical
des	Destruction
en	Energy
ex	Exergy
helio	Heliostat
inc	Incident
ph	Physical

substantial increase in the H_2 concentration, which was elevated from 23 % mol to 80 % mol on a dry basis. Osat et al. [8] presented a chemical plant for the conversion of rice straw into biofuels via a SEG process. The proposed system achieved the production of 222.6 tons of butanol and 960 tons of pentanol as products per day. The evaluation of SEG for H_2 production from municipal solid waste (MSW) was carried out by Santos and Hanak [5]. They conducted a comparison with conventional gasification. The study findings indicated that while the SEG system demonstrated superior environmental performance, it was accompanied by elevated costs that necessitated reductions for enhanced competitiveness. Zhang et al. [9] presented a customized system presented a customized system designed to produce H_2. This system integrated CaL and methane (CH_4) reformer methods. Their investigation findings highlighted a significant increase in H_2 production attributed to the incorporation of methane reforming. All of these studies were conducted to achieve a sustainable energy system with efficient performance and the lowest environmental impact.

Odum [10] identified the biosphere as the primary source of resources and environmental services, all powered by solar energy. Following this recognition, emergy analysis emerged as a method for evaluating the sustainability and environmental impacts of energy systems. Several studies have applied emergy analysis to power generation cycles. For instance, Brown and Ulgiati [11] evaluated six electricity generation systems using energy and emergy analysis and compared their performance. Zhang et al. [12] performed emergy analysis for an Organic Rankine Cycle and investigated its sustainability. Their findings revealed that the designed system, boasting a sustainability index of 3.97, surpassed the performance of fossil fuel plants. Paoli et al. [13] identified the challenge of improving the efficiency and competitiveness of renewable energy sources compared to non-renewables in terms of environmental impact. They applied emergy analysis to evaluate sustainability and found that solar technologies offer significant energy savings. This research advocates for the utilization of solar energy as a means to conserve non-renewable energy sources. Yazdani et al. [14] conducted a comprehensive analysis using emergy assessment to evaluate the sustainability of two different power generation systems. The sustainability index was 1.65 for the biomass-based system and 0.05 for the natural gas-fueled configuration. Jalili et al. [15] performed an emergy analysis and multi-objective optimization for a combined electricity and freshwater generation system in two different states. The results revealed that under optimum operating conditions when the system is exclusively fueled by biomass, it exhibits higher sustainability compared to when co-fueled with natural gas and biomass.

Utilizing response surface methodology (RSM) proves to be a valuable approach for conducting multi-objective optimization. RSM is extensively utilized in various engineering fields where the optimization of multiple objectives simultaneously is necessary. RSM provides a structured and efficient framework for modeling and optimizing complex processes. Its capability to optimize multiple responses concurrently makes it particularly suitable for tasks involving multi-objective optimization. Some studies have employed this method to optimize the performance of various processes, such as steam gasification [16], emissions in diesel engines [17], photovoltaic/thermal (PVT) systems [18], and CO_2 capture by potassium hydroxide-modified activated alumina [19], among others. A limited number of studies have utilized RSM in energy systems that encompass the integration of various processes. Mojaver et al. [20] employed RSM to optimize an integrated system comprising biomass gasification, solid oxide fuel cell (SOFC), and high-temperature sodium heat pipes. The results indicated that the regression models were accurate, achieving an exergy efficiency of 42.22 % and power generation of 535 kW under optimum conditions. Roy et al. [21] applied RSM for the multi-objective optimization of SOFC and the integration with a supercritical carbon dioxide cycle for power generation. The optimization results indicate that the system achieves optimum performance at an energy efficiency of 64 %. Sun et al. [22] introduced a novel co-generation system configuration involving the Kalina cycle and proton exchange membrane electrolyzer, employing the RSM method for optimization. The adjusted regression coefficients for the sum unit cost of the product and exergy efficiency, considered as objectives of the system, were reported as 98.4 and 97.6, respectively. At

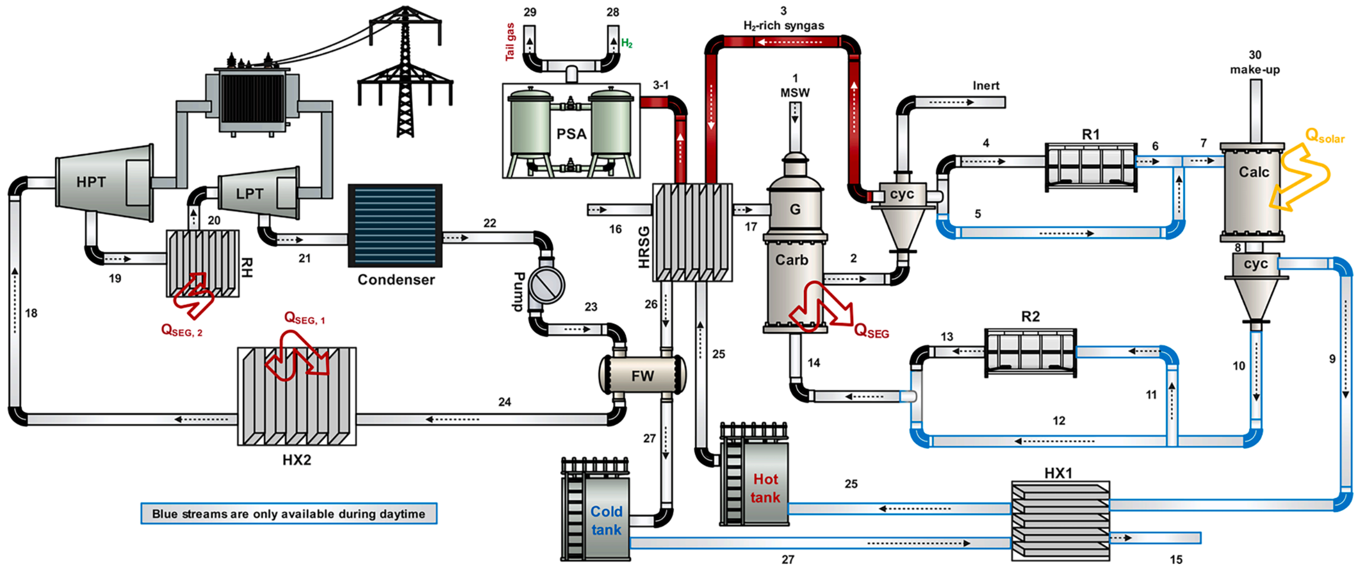

Fig. 1. Schematic of the integration of solar-based SEG system with waste heat recovery system.

the optimum point, a main product unit cost of 1.75 \$/h and an exergy efficiency of 31.71 % were determined. Pourali and Esfahani [23] explored a novel combined system for H_2 production and enhanced its efficiency through the application of RSM. For five optimized designs of the integrated system, the energy efficiency has been optimized to be greater than 80 %.

The existing literature reveals a significant research gap concerning the integration of SEG systems with waste heat recovery cycles, sustainability assessments, and performance optimization. While numerous studies have investigated SEG utilizing various feedstocks, comprehensive research specifically evaluating the viability, efficiency, and environmental impact of SEG-integrated energy systems remains scarce. Although some studies have employed methodologies such as RSM, emergy analysis, and energy analysis separately for different types of systems, there is a notable absence of a holistic energy, economic, and environmental analysis for MSW-driven SEG-integrated energy systems.

This study aims to address gaps in the field by conducting an emergy analysis of an H_2 and electricity generation system using a solar-based SEG process, applying RSM for optimization, and investigating critical parameters influencing the overall system efficiency. The study makes significant contributions in the following aspects:

1) Developing a conceptual framework for an integrated system that combines a solar-based SEG process with a waste heat recovery system.
2) Conducting thorough analyses, including techno-economic, exergy, and emergy assessments of the whole system.
3) Performing a comprehensive sensitivity analysis on key design parameters, focusing on energy, exergy, and the levelized cost of energy.
4) Undertaking a study using RSM to achieve optimal performance for the integrated system through multi-objective optimization.

2. Model development and methodology

2.1. System description

Fig. 1 shows the schematic of the proposed system, which starts with MSW gasification in the gasifier reactor. After producing the syngas, it enters the carbonator reactor, along with the solid sorbent (state 14), to separate CO_2 through the CaL process. The gasifier and carbonator reactors serve as the two-staged reactor, called SEG reactor. Upon removing CO_2, the products (state 2) pass through the cyclone, separating into two streams: solid and gas. The gas stream is the syngas, which has captured a significant amount of CO_2 from its composition. Solid materials include the formed $CaCO_3$ from the capture process and deactivated sorbents. The deactivated materials separate from this $CaCO_3$ as inert, and the remaining solid components are further divided into two states (states 4 and 5). The first part is stored in reservoir 1 (R1), and the second part is transferred to the calciner to revive CaO in an endothermic process.

Reservoir 1 is instrumental in fulfilling the solar energy requirements of the calciner reactor, effectively addressing the limitations posed by solar radiation. It stores solid materials during the night and transfers them to the calciner during the day, in accordance with solar radiation, and the absorbed heat by the calciner from the solar field.

In the calciner reactor, after regenerating the sorbent through the calcination reaction, products (state 8) enter a cyclone to separate the regenerated sorbent from the captured CO_2. Regenerated sorbent splits into two streams, with the first one stored in reservoir 2 (R2), and the second one going to the carbonator reactor directly. This storage process is designed to retain surplus regenerated sorbent and transport it to the carbonator reactor during periods of insufficient solar radiation when the required amount is not met.

The SEG cycle makes it possible to integrate with a waste heat recovery system due to the availability of high-temperature heat sources:

I. Released heat from the SEG reactor.
II. Produced syngas at high temperature.
III. Captured CO_2 at high temperature.

As a result, a waste heat recovery cycle is being considered to utilize these available heat sources. Given that captured CO_2 is accessible throughout sunlight hours, a heat storage system is being designed to continually store its thermal energy. This enables the continuous use of stored heat in recovery and secondary cycles, whether day or night. In this regard, two storage tanks are employed, and liquid sodium passes through HX1, absorbing thermal energy from CO_2, becoming hot, being stored in the hot tank, and being available in a steady state as a heat source. The produced syngas (state 2) is used as a heat source in a heat recovery steam generator (HRSG) to produce superheated steam as a gasification agent from the water at ambient temperature. Liquid sodium in the high-temperature tank is also utilized as an extra source of thermal energy in the HRSG. A reheated steam cycle is also considered as a secondary power cycle, driven by the heat discharged from the SEG process as the main heat source and the remaining thermal energy from

Table 1
Properties of MSW [5].

Element composition ($\%_{wt}$)					**LHV (MJ/kg)**
C	O	H	N	S	
49.51	35.69	6.42	0.78	0.48	19.99
Moisture content ($\%_{wt}$)	**Volatile matter ($\%_{wt}$)**				
9.34	77.52				
Fixed carbon ($\%_{wt}$)	**Ash ($\%_{wt}$)**				
15.36	7.12				

the hot liquid sodium (state 26) as a feedwater heater heat source. After imparting its thermal energy, the syngas stream enters a pressure swing adsorption unit (PSA) to distinguish the H_2 among the remaining gases.

2.2. Gasification process

The SEG process design incorporates solar-driven CaL for capturing CO_2 on-site, involving the capture of CO_2 during the gasification of MSW to produce H_2-rich syngas. The following assumptions have been considered for modeling the gasification and syngas production process [5,24,25]:

- The gasification is carried out using steam as the agent at a temperature of 350 °C.
- Negligible consideration is given to changes in energy potential and kinetic states.
- The creation of tar is overlooked.
- The compositions of the syngas are regarded as ideal gases.

The modeling of the gasification process was achieved using a thermodynamic equilibrium approach, considering the global gasification reaction [26]:

$$CH_xO_yN_z + (\omega+\varepsilon)H_2O \rightarrow n_{H_2}H_2 + n_{CO}CO + n_{CO_2}CO_2 + n_{H_2O}H_2O + n_{CH_4}CH_4 + n_{N_2}N_2 \quad (1)$$

In the global reaction, x, y, and z represent the molar ratios of each corresponding atom to carbon and can be established by performing an ultimate analysis, as outlined in Table 1. Additionally, the ratio of moisture to dry ash-free MSW can be expressed as [25]:

$$\omega = \frac{(M_{MSW} \times MC)}{M_{H_2O} \times (1-MC)} \quad (2)$$

where MC signifies the moisture content in the biomass, and M stands for the molecular mass. To determine the six unknowns in Equation (1), six equations are needed. Four equations can be written from the atom balance in this reaction for C, H, O, and N. Additionally, two supplementary equations can be established in accordance with the equilibrium constant relationships, which pertain to intermediate reactions occurring during the gasification process. The methodology employed for this purpose is detailed in prior research conducted by the authors of this study [27].

2.3. Solar-based CaL

In this system, CaL is employed as an on-site capture process for the removal of CO_2 from the produced syngas. The CO_2 capture takes place in the second stage of the SEG reactor, known as the carbonator, through the carbonation reaction, which is described as follows [28]:

$$CaO + CO_2 \rightarrow CaCO_3 \Delta H = -178 kJ/mol \quad (3)$$

CaO serves as the sorbent, reacting with CO_2 to form $CaCO_3$ in this process.

Table 2
Operation conditions of the capture process [32].

Parameter	$\frac{F_0}{F_{CO_2}}$	Sorbent regeneration rate	Carbonator temperature	Calciner temperature
Value	0.1	100 %	650 °C	900 °C

The carbonation reaction is exothermic, releasing a significant amount of heat that can be utilized in waste heat recovery cycles. Additionally, a portion of this heat can provide the required heat to initiate the gasification process [29]. To maintain a continuous loop for capturing CO_2 and regenerating the sorbent, $CaCO_3$ is transferred to the calciner reactor, where it decomposes into CO_2 and CaO through the calcination reaction as follows [28]:

$$CaCO_3 \rightarrow CaO + CO_2 \Delta H = 178 kJ/mol \quad (4)$$

The calcination reaction requires a heat source as it is an endothermic process. In this study, to enhance overall performance and utilize renewable energy sources, a heliostat field is utilized to supply heat to the calciner reactor. In this context, the calciner is designed as an outer receiver that harnesses and makes use of sunlight redirected by the mirrors. The heat supplied through the solar field, which is absorbed by $CaCO_3$ to facilitate decomposition and sorbent regeneration, can be calculated by Equation (5) [30]:

$$\dot{Q}_{abs} = \eta_{helio}\dot{Q}_{inc} \quad (5)$$

where $\dot{Q}_{inc}$ represents the incident heat flow rate, and Î·$_{helio}$ stands for the heliostat field efficiency. Earlier research, conducted by the authors of this study, provides the detailed design of the heliostat field [31].

Efficiency in capturing CO_2 is a vital element in the CaL process, contingent upon numerous variables, including the sorbent ratio and sorbent activity. Capture efficiency can be expressed as follows:

$$E_{carb} = min\left(\frac{F_R X_{ave}}{F_{CO_2}}, E_{equil}\right) \quad (6)$$

In Equation (6), E_{equil} represents the CO_2 fraction captured by the sorbent in equilibrium conditions, while F_R and F_{CO2} denote the flow rate of CaO and CO_2, respectively. The calculation of the average fraction of active CaO is outlined in reference [32]:

$$X_{ave} = \frac{f_m(1-f_w)F_0}{F_0 + F_R(1-f_m)} + f_w \quad (7)$$

The average fraction of active CaO depends on two fixed factors, represented by f_m and f_w, which are associated with the characteristics of the CaO. In this case, these values are 0.77 and 0.17, respectively [32]. Table 2 summarizes the design parameters and operation conditions of the designed CaL.

The following assumptions have been considered to simulate the CaL process and integrate it with the gasifier [5,31]:

- Carbonation reaction takes place continuously, both day and night.
- The calcination reaction occurs in the presence of solar radiation
- It is presumed that the reservoirs have insulation.

The SEG reactor, an integration of the gasifier and carbonator reactor, must be maintained at a temperature of 650 °C to meet the requirements of the carbonation reaction.

2.4. Heat recovery and thermal energy storage unit

The integrated SEG system offers substantial heat recovery potential thanks to the exothermic reaction within the carbonator and the high-temperature streams (produced syngas and captured CO_2) exiting the SEG system. HRSG 1 is used to produce super-heated steam for the

Table 3
Design parameters of the waste heat recovery cycle.

Parameters	Value	Unit
Î·$_{iso_{HPT}}$ [33]	90	%
Î·$_{iso_{LPT}}$ [33]	90	%
Î·$_{P}$ [33]	80	%
ΔAP_{HRSG} [34]	20	℃
P_{cond} [33]	0.1	Bar

gasification process, and a secondary power generation cycle is coupled with the enhanced gasification process to harness the available heat sources and generate electrical power. To overcome the constraint of separated CO_2 availability only with solar radiation, two isolated storage tanks are utilized. This storage system is charged during the day and discharged at night, ensuring a continuous and steady heat source for the Rankine cycle throughout the day. Table 3 showcases the design parameters of the waste heat recovery system.

The following assumptions served as the basis for simulating the waste heat recovery system [35–37]:

- Liquid sodium has been chosen as the working fluid for the thermal energy storage tanks.
- Storage tanks are assumed adiabatic.
- Pressure drop is neglected in heat exchangers and pipelines.
- Rankine cycle and HRSG 1 operate in steady-state condition.

3. Performance evaluation

In this section, an analysis of the proposed system is provided from multiple viewpoints, including energy, exergy, emergy, and economic aspects. The simulations and analyses were carried out using EES software, which was also linked with TRNSYS software to calculate the solar radiation and absorbed heat.

3.1. Energy and exergy analyses

The designed process was analyzed by applying the first law of thermodynamics to individual components, in the following manner [38]:

$$\sum_{in}\dot{m} = \sum_{out}\dot{m} \tag{8}$$

$$\dot{Q} - \dot{W} + \sum_{in}\dot{m}\left(h + \frac{V^2}{2} + gZ\right) - \sum_{out}\dot{m}\left(h + \frac{V^2}{2} + gZ\right) = \frac{dE}{dt} \tag{9}$$

The performance of the system can be evaluated from an energy perspective using the following equation:

$$\eta_{en} = \frac{\dot{W}_{net} + (\dot{m}_{H_2}LHV_{H_2}) + (\dot{m}_{tail}LHV_{tail})}{(\dot{m}_{MSW}LHV_{MSW}) + \dot{Q}_{solar}} \tag{10}$$

In this definition, the energy efficiency of the proposed system is described as the ratio of the total generated energy rate (including electrical power and syngas production) to the total input energy rate in the system, which comes from biomass and solar radiation.

To apply the second law of thermodynamics to each control volume in the presented system at steady-state operating conditions, the exergy balance can be written as [34]:

$$\sum_{in}\dot{E}x = \sum_{out}\dot{E}x + \dot{E}x_{des} \tag{11}$$

Exergy may manifest in different forms. The computation of exergy for the processes associated with heat is carried out by the following equation [39]:

$$\dot{E}x_Q = \dot{Q}\left(1 - \frac{T_0}{T_{Source}}\right) \tag{12}$$

the summation of both the chemical and physical exergies associated with a specific stream [40]:

$$ex = ex_{ph} + ex_{ch} \tag{13}$$

The physical exergy, representing the distinction between the stream condition and the dead state, is calculated as follows [41]:

$$ex_{ph} = (h - h_0) - T_0(s - s_0) \tag{14}$$

The chemical exergy of the ideal gas mixture and MSW is described by the respective equations [42,43]:

$$\dot{E}x_{ch}^{mixture} = \sum_i \dot{n}_i\left(ex_{chi} + RT_0 ln\frac{\dot{n}_i}{\sum \dot{n}_i}\right) \tag{15}$$

$$Ex_{MSW} = \beta LHV_{MSW} + MC(ex_{chw} + \beta h_{vap}) \tag{16}$$

Table 4
PEC functions of integrated system components.

Component	PEC Function	Year	Convertibility	Ref
Gasifier	$1600\left(3600\dot{m}_{MSW}\right)^{0.67}$	2008	596.2/575.4	[25]
Heliostat field	$75(A_{helio})$	2020	596.2/596.2	[27]
Carbonator	$10^6(0.2882\dot{Q}_{carb}[MW_{th}] + 5.0874)$	2014	596.2/576.1	[27]
Calciner	$10^6(0.2564)\left(\dot{Q}_{in}[MW_{th}]\right)^{0.65}$	2014	596.2/576.1	[27]
PSA	$10^6(27.96)\left(\frac{\dot{n}\,[\frac{kmol}{s}]}{17069}\right)^{0.6}$	2020	596.2/596.2	[5]
Pump	$3540\dot{W}_P^{0.71}$	2011	596.2/585.7	[25]
Condenser	$10^6(6.988)\left(\frac{\dot{Q}_{cond}[MW_{th}]}{290}\right)^{0.8}$	2018	596.2/603.1	[47]
Reservoir	$10^6(1.4219)\left(\frac{volume}{500}\right)^{0.4446}$	2018	596.2/603.1	[3]
HX	$10^6(2.617\times10^{-3})(A)^{0.69}(p)^{0.28}$	2005	596.2/468.2	[27]
Turbine	$10^6(37.06)\left(\frac{gross\ power\ [MW]}{263}\right)^{0.8}$	2018	596.2/603.1	[27]

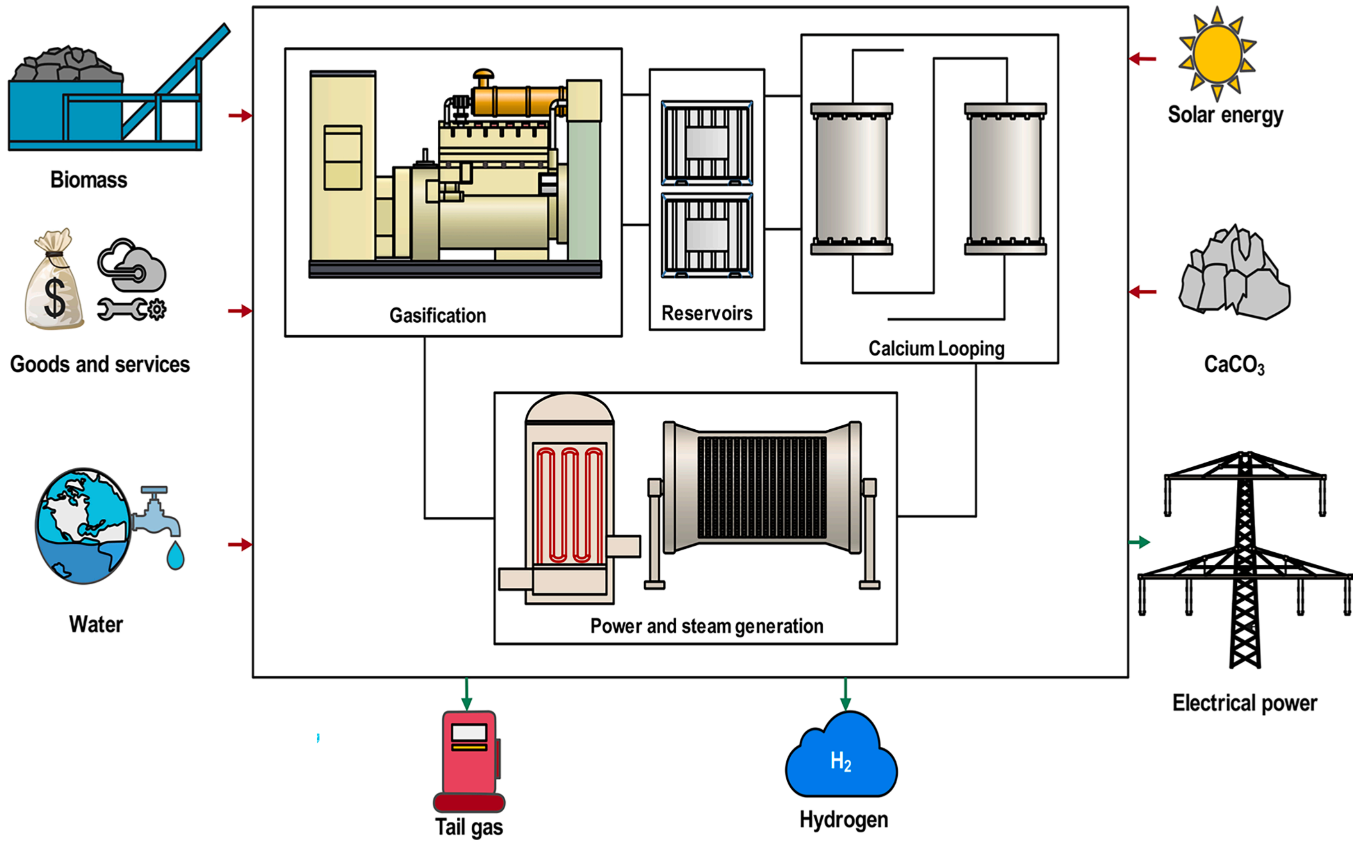

Fig. 2. Emergy diagram for the proposed system.

The symbol β, as a correlation factor, is given by [43]:

$$\beta = \frac{1.044 + 0.016(H_C) - 0.3493(O_C)(1 + 0.0531(H_C)) + 0.0493(N_C)}{1 - 0.4124(N_C)} \tag{17}$$

H_C, N_C, and O_C in the MSW represent the atomic fraction in the biomass. From an exergy point of view, the efficiency for the components and integrated system is determined by[44]:

$$\eta_{ex} = 1 - (\frac{\dot{Ex}_{des}}{\dot{E}_{in}}) \tag{18}$$

3.2. Economic analysis

The economic performance of the proposed system is indicated by calculating the levelized cost of energy (LCOE). This metric is defined as the ratio of the total system cost to net power and syngas production (including H_2 and tail gas). It can be formulated as [25]:

$$LCOE = \frac{Totalcost}{Totalpoweroutputsofthesystem} \tag{19}$$

Both the capital investment cost rate (C_k^{CI}) and the operation and maintenance cost rate (C_k^{OMC}) of the components constitute the total cost rate (C_K) of the system. It can be calculated through Equation (20) [45]:

$$C_k = C_k^{CI} + C_k^{OMC} = \frac{(PEC_k CRF\varphi)}{N} \tag{20}$$

The procurement cost for each component, denoted as PEC in US dollars, is a representation of the cost associated with the acquisition of each element. Table 4 outlines the PEC function corresponding to each component. The total annual operational hours for the system are represented by N, and the assumed cost equivalent coefficient for system operation and maintenance, set at 1.06 for this study, is denoted by φ. The capital recovery factor, abbreviated as CRF, can be calculated using the provided equation [46]:

$$CRF = \frac{i(1+i)^{BL}}{(1+i)^{BL} - 1} \tag{21}$$

where i is the interest rate, and BL stands for the life time of the system.

3.3. Emergy analysis

Emergy analysis is a concept that examines the differences in the quality of various types of energy, and this approach is used for the sustainability analysis of energy systems. Basically, emergy denotes the utilization of a specific quantity of energy, either directly or indirectly, in the processes involved in producing a product or service [10,48]. In evaluating the sustainability of a system, multiple inputs, including energy, work, air, money, etc., are considered. The initial stage involves standardizing all these inputs into a common unit. In emergy analysis, where solar energy serves as the primary source for all energies and resources within the biosphere, whether directly or indirectly, the conversion of all inputs is performed using a unit referred to as solar emjoules (seJ). Emergy analysis consists of fundamental steps. Firstly, defining the system boundary and specifying all inputs, with a particular emphasis on energy analysis, is paramount. Once all inputs are identified, the subsequent stage involves converting them to solar seJ using established conversion factors documented in the literature. Finally, armed with information gathered through the preceding steps, emergy indexes can be computed to provide a comprehensive assessment of the system [15,49]. The total emergy input of a system can be calculated as follows [15]:

$$Y = R + N + F \tag{22}$$

Table 5
Emergy indices calculated for the present system [15].

Index	Formula
Emergy yield ratio (EYR)	$EYR = \frac{Y}{F}$
Renewability (%R)	$\%R = \frac{R}{Y}$
Emergy investment ratio (EIR)	$EIR = \frac{F}{R+N}$
Environmental load ratio (ELR)	$ELR = \frac{1\text{-}\%R}{\%R}$
Emergy sustainable index (ESI)	$ESI = \frac{EYR}{ELR}$

In the given context, R stands for local- renewable sources, N denotes local non-renewable sources, and F signifies economic inputs.

Fig. 2 illustrates the emergy diagram for the proposed system, while Table 5 presents key information on the emergy indices utilized in this study. The system boundary, emergy inputs, products of the system, and the concept of each index are elaborated in the figure and table, offering a detailed understanding of the study's essential components.

The indices presented in Table 5 can be defined and explained as follows:

- Emergy yield ratio (EYR)

The EYR index represents the dependency of the system on economic inputs and is defined as the ratio of the total emergy input (Y) to economic inputs (F). A higher EYR index implies that the analyzed system has the lowest dependency on economic inputs.

- Renewability (%R) index

The %R index functions as a renewability indicator, quantifying the proportion of local renewable sources (R) in relation to the total emergy inputs to the system (Y). A lower value indicates a reduced reliance on non-renewable sources.

- Emergy investment ratio (EIR)

The EIR index is crucial for evaluating investment factors as it assesses the system's ability to acquire inputs from external, non-local sources (economic inputs) in comparison to local sources, which include both renewable and non-renewable resources. This index is defined as the ratio of economic inputs (F) to the combined sum of non-renewable and renewable local sources.

- Environmental load ratio (ELR)

A high ELR index implies greater reliance on economic and non-renewable sources, resulting in severe environmental impacts. An ELR index approximately at 2 implies a minimal environmental impact, whereas values falling between 3 and 10, or surpassing 10, signify moderate and significant environmental impacts, respectively.

- Emergy sustainable index (ESI)

The ESI is defined as the ratio of the two most important indices (EYR/ELR), making it the cornerstone of emergy analysis. It seamlessly integrates economic and environmental considerations, rendering it the most pivotal index in the assessment. This index specifies the sustainability of the system. An ESI below 1 indicates that the system is not sustainable, an ESI index between 1 and 5 suggests the system is medium-term sustainable, and an ESI above 5 means that the system is totally sustainable.

Table 6
RMS Error between developed model and study findings in References [5,52].

SB	RMS Error (syngas composition)
0.5	3.85
0.6	2.26
0.7	2.2
0.8	2.66
0.9	2.72
1	3
Gas composition	**RMS Error (H_2-rich syngas composition)**
H_2	0.97
CO_2	0.024
CO	0.121
CH_4	0.87

3.4. Response surface methodology (RSM)

This study used RSM to establish a link between desired outcomes and defined input factors. Additionally, it examined how the chosen input variables interacted to influence the desired outcomes. This method was employed to create the numerical experiment layout [21]. The numerical design is established using the Box-Behnken experimental design method, pioneered by George E. P. Box and Donald Behnken [50]. CO_2 capture efficiency (CE) and the steam-to-biomass ratio (SB) were designated as input variables, while total energy efficiency (η_{en}), exergy efficiency (η_{ex}), and levelized cost of electricity (LCOE) were chosen as the objective responses. The intricate connections between the objective responses and input variables are encapsulated in the comprehensive quadratic model, expressed as follows [51]:

$$Y_i = a_0 + \sum_i^k a_i X_i + \sum_i^k a_{ii} X_i^2 + \sum_i^{k-1} \sum_j^k a_{ij} X_i X_j + e1 \leq i \leq kj = i+1 \tag{23}$$

In this context, Y_i represents the response, X stands for the factor, k denotes the number of factors, and a coefficient is the corresponding coefficients in the regression equation with unknown values.

4. Results and discussion

The entire system underwent analyses encompassing energy, exergy, economic, and emergy aspects. The application of RSM is employed to further investigate and optimize the system's performance. The outcomes of these analyses are elaborated in this section.

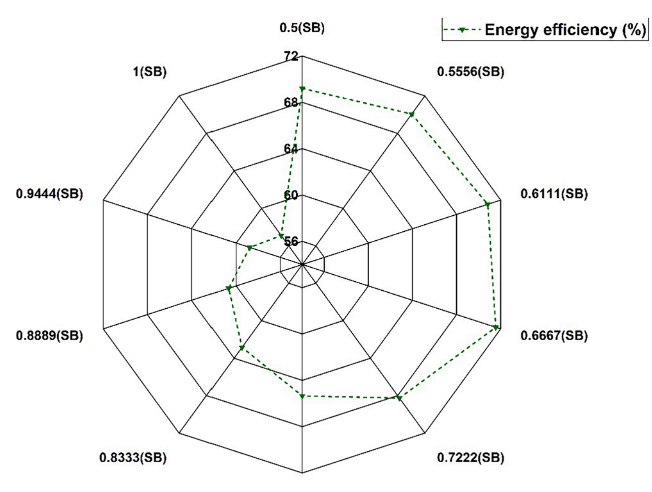

Fig. 3. Effect of the SB on the total energy efficiency.

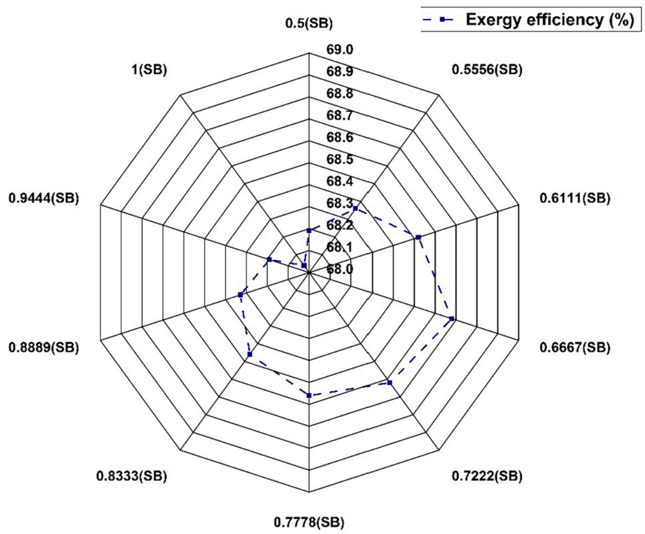

Fig. 4. Effect of the SB on the exergy efficiency.

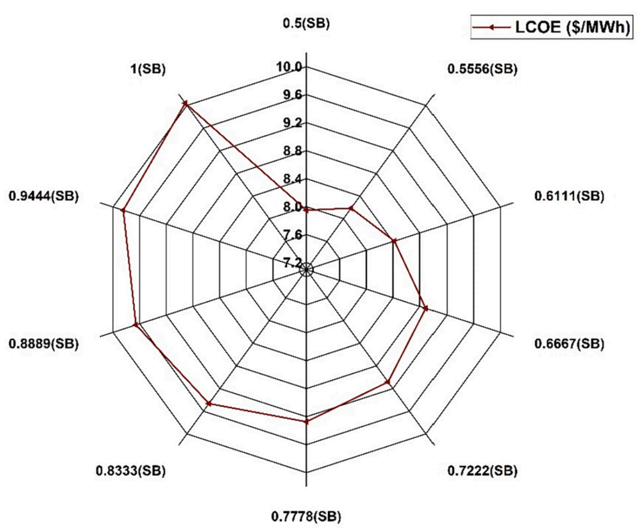

Fig. 5. Effect of the SB on the LCOE.

4.1. Model validation

The outcomes of both the gasification and SEG procedures have undergone validation and verification through references in the available literature [5,52]. The differences between the simulated and experimental data are detailed in Table 6, assessed through the calculation of root-mean-square (RMS) values. The resulting RMS values indicate that the model developed in this study accurately predicts the syngas composition, providing a satisfactory approximation to the experimental data. Moreover, following the SEG process, the composition of H_2-rich syngas aligns well with the model developed by Santos and Hanak [5].

4.2. Sensitivity analysis

The variation in the three objectives of the proposed system, introduced in the previous section, has been investigated in conjunction with the parameters of SB and CE. SB and CE, as independent parameters within the proposed system, significantly influence the overall system performance. The results of the sensitivity analysis can be utilized in the RSM to optimize and enhance the overall system performance. Fig. 3

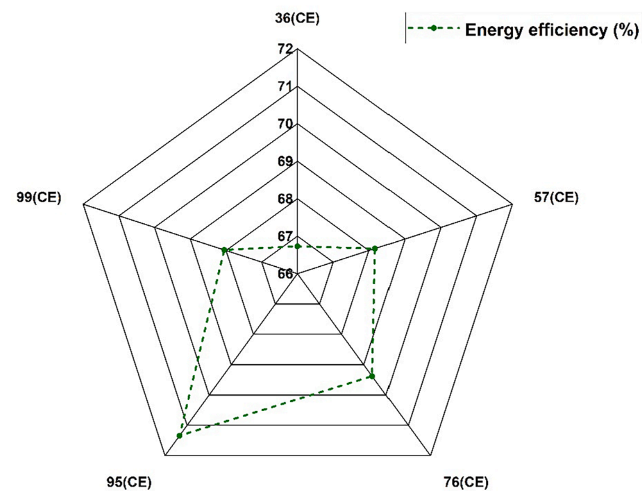

Fig. 6. Effect of the CE on the total energy efficiency.

illustrates the impact of the SB on the total energy efficiency of the proposed system. The energy efficiency of the entire system increases with an elevation in the SB, reaching its peak value at an SB of 0.667. Beyond this ratio, the system experiences a decline in energy efficiency. Despite the increase in net power and H_2 generation rates, there is a significant rise in heat demand within HRSG and the calciner reactor. The impact of this heightened heat demand on the reduction in energy efficiency is more noticeable than the effect on net power generation.

Fig. 4 depicts the impact of SB on the efficiency of the system in terms of exergy. As the steam quantity increases in the gasification process, there is a decrease in exergy destruction in the carbonator and gasifier. Conversely, an increased steam supply gives rise to greater exergy destruction in the calciner reactor, power cycle, and HRSG. Particularly, the waste heat recovery system, especially within the HRSG, undergoes a significant upsurge in exergy destruction when the steam supply is augmented. The overall escalation in exergy destruction in the calciner reactor and waste heat recovery system outweighs the reduction in exergy destruction in the carbonator reactor and gasifier. This results in a decline in exergy efficiency as the steam supply increases. According to Fig. 5, higher SB are expected to yield the highest total cost rates in the entire system. The rise in costs associated with equipment size, especially in the calciner reactors, contributes to the overall increase, requiring a larger heliostat field area. This cost escalation surpasses the growth in system output, resulting in a LCOE with increasing SB.

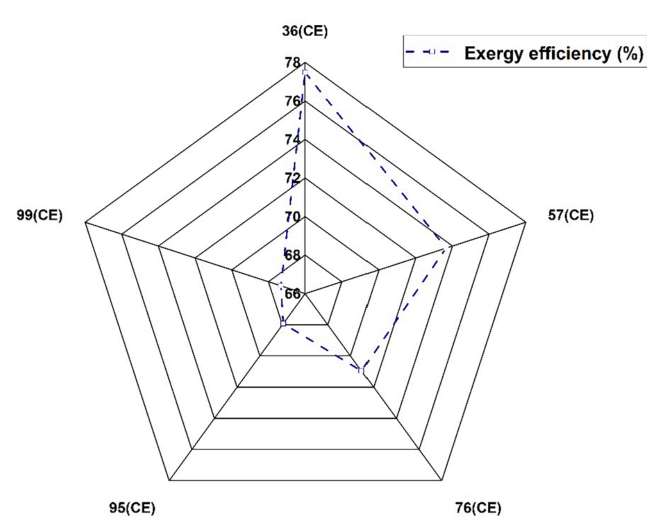

Fig. 7. Effect of the CE on the exergy efficiency.

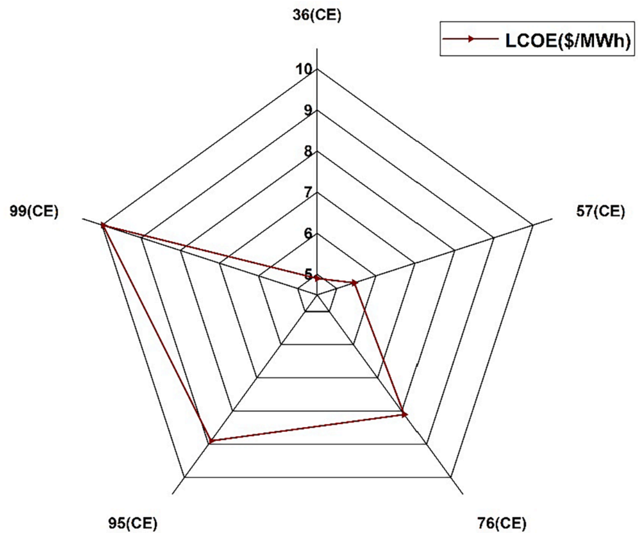

Fig. 8. Effect of the CE on the LCOE.

Table 7
Analysis of variance for the proposed system.

Source	DF	Adj SS	Adj MS	F-Value	P-Value
Energy Efficiency					
Model	4	190.715	47.679	47.35	<0.0001
Linear	2	173.529	86.764	86.17	<0.0001
SB	1	172.685	172.685	171.50	<0.0001
CE	1	0.843	0.843	0.84	0.387
Square	2	17.186	8.593	8.53	0.010
SB*SB	1	13.538	13.538	13.44	0.006
CE*CE	1	5.635	5.635	5.60	0.046
Error	8	8.056	1.007		
Lack-of-Fit	4	8.056	2.014	*	*
Pure Error	4	0.000	0.000		
Total	12	198.771			
Exergy Efficiency					
Model	3	11.9610	3.98701	75.62	<0.0001
Linear	2	10.6696	5.33482	101.19	<0.0001
SB	1	2.9166	2.91664	55.32	<0.0001
CE	1	7.7530	7.75300	147.05	<0.0001
Square	1	1.2914	1.29138	24.49	0.001
SB*SB	1	1.2914	1.29138	24.49	0.001
Error	9	0.4745	0.05272		
Lack-of-Fit	5	0.4745	0.09490	*	*
Pure Error	4	0.0000	0.00000		
Total	12	12.4355			
LCOE					
Model	2	1.92916	0.96458	47.53	<0.0001
Linear	2	1.92916	0.96458	47.53	<0.0001
SB	1	1.18003	1.18003	58.14	<0.0001
CE	1	0.74913	0.74913	36.91	<0.0001
Error	10	0.20295	0.02030		
Lack-of-Fit	6	0.20295	0.03383	*	*
Pure Error	4	0.00000	0.00000		
Total	12	2.13211			

The CE is influenced by variations in both CaO to CO_2 and make-up to CO_2 ratios values. As the second ratio increases, there is a need to introduce a higher quantity of fresh $CaCO_3$ in the makeup flow. This results in elevated energy consumption and additional expenses [32]. Consequently, this study opts to boost the CE parameter by deliberately raising the CaO to CO_2 ratio (F_R/F_{CO2}). Illustrated in Fig. 6, the energy efficiency of the system demonstrates an upward trend with the rise in CE, reaching its maximum at a CE of 95 %. Beyond this capture rate, the F_R/F_{CO2} experiences a sharp increase owing to CaL characteristics. This implies a heightened demand for heat in the $CaCO_3$ decomposition process within the decomposition reactor (clciner), consequently elevating the overall energy input to the system. The magnitude of this increase surpasses the energy output across the entire system, leading to an anticipated decline in energy efficiency beyond this specific CE rate.

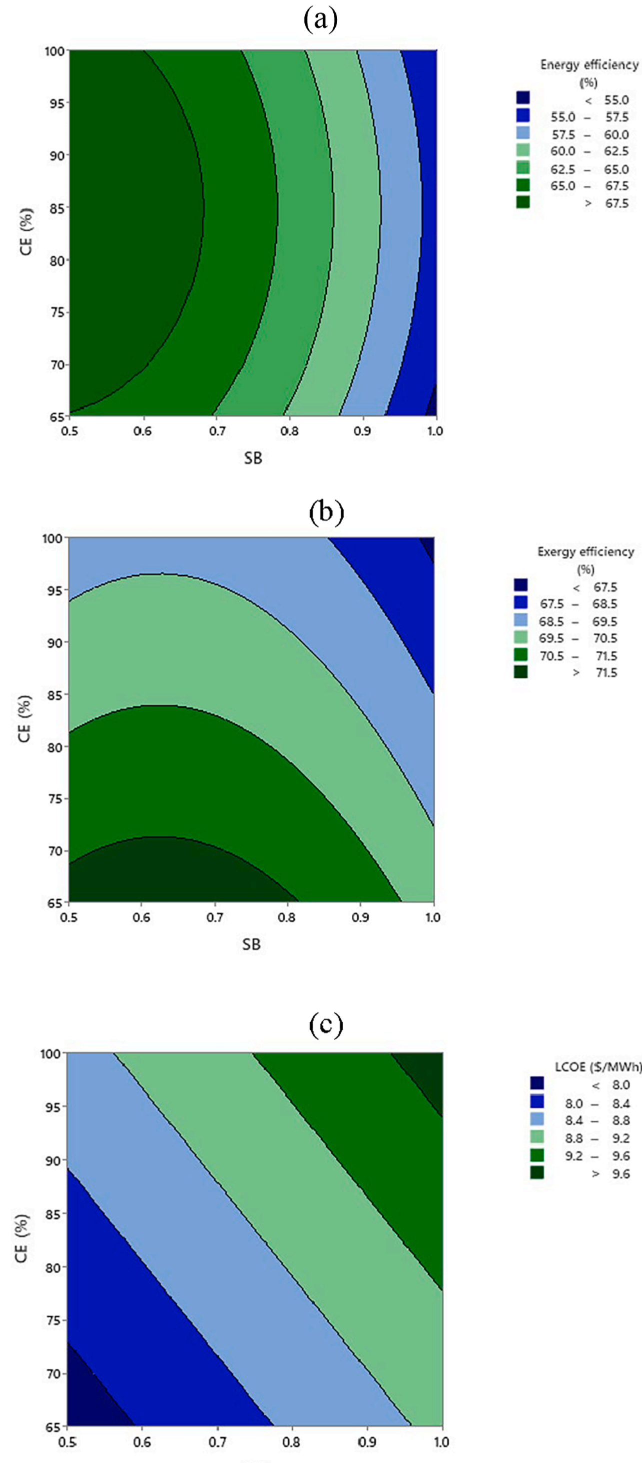

Fig. 9. Interaction effect of SB and CE on: a) energy efficiency; b) exergy efficiency; and c) LCOE.

With a rise in sorbent molar rate at high CE, there is an increased demand for heat in the calcination process within the calciner reactor. Essentially, there is a rise in exergy destruction throughout, leading to a decline in exergy efficiency. This is evident in Fig. 7. Fig. 8 illustrates a direct correlation between LCOE and CE. The pursuit of higher CE necessitates an expanded calcination process in the reactor, contributing to

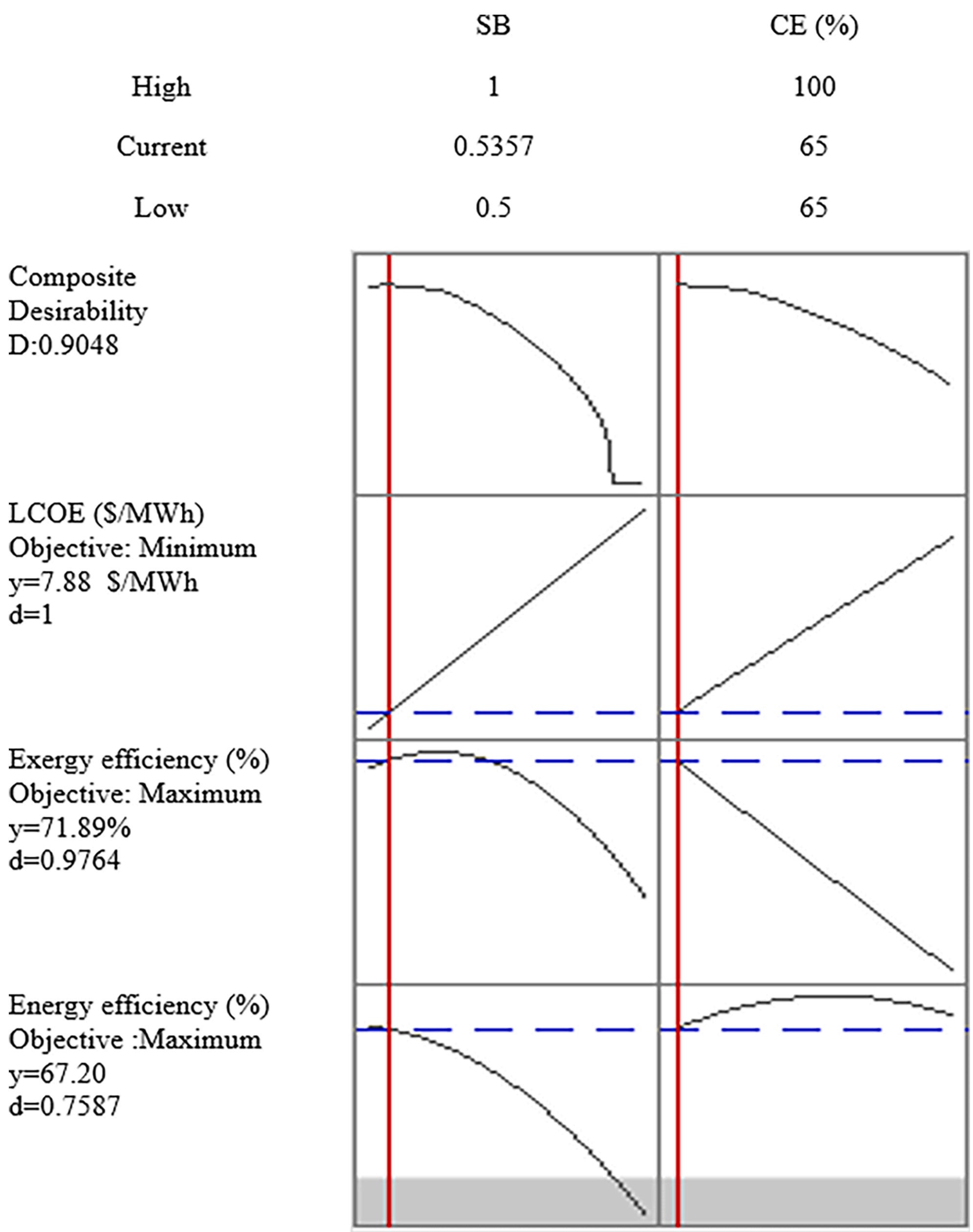

Fig. 10. Response optimizer plot.

the enlargement of the heliostat field area. Anticipating that the costs associated with the solar system form a substantial part of the total expenses, an upturn in LCOE is anticipated.

4.3. RSM and multi-objective optimization

Regression equations for the system's three objectives have been developed, and they are presented below:

$$\text{Energy efficiency}\,(\%) = 18.3 + 40.7\,\text{SB} + 0.996\,\text{CE} - 44.6\,\text{SB}^2 - 0.00588\,\text{CE}^2 \tag{24}$$

$$\text{Exergy efficiency}\,(\%) = 71.83 + 17.09\,\text{SB} - 0.07955\,\text{CE} - 13.67\,\text{SB}^2 \tag{25}$$

$$\text{LCOE}\,(\$/\text{MWh}) = 5.107 + 2.173\,\text{SB} + 0.02473\,\text{CE} \tag{26}$$

The results of the analysis of variance for the three system objectives are depicted in Table 7. Across all objectives, the p-value for each of the three models is significant, and notable F-values are observed for all three objectives. This provides strong evidence of the model's significance. A P-value above 0.05 suggests support for the null hypothesis, while a statistically significant result ($P \leq 0.05$) indicates rejection of the test hypothesis [21].

In Fig. 9, the interaction effects of CE and SB on the proposed system's objectives are illustrated. It is evident that the highest total energy is achieved at a low value of SB, emphasizing SB's predominant influence on energy efficiency. Conversely, the maximum exergy efficiency is attained at a low value of CE, highlighting CE's primary impact on exergy efficiency. Additionally, a low value of LCOE is noted when both SB and CE are at low levels, indicating their combined effect on LCOE. These findings underscore that energy efficiency is most substantially affected by SB, while exergy efficiency is most impacted by CE. This pattern is substantiated by the simultaneous increase in CE and SB, resulting in higher total system costs that outweigh the gain in generated energy, leading to an increase in LCOE. From an exergy standpoint, higher CE values contribute to increased exergy destruction in the

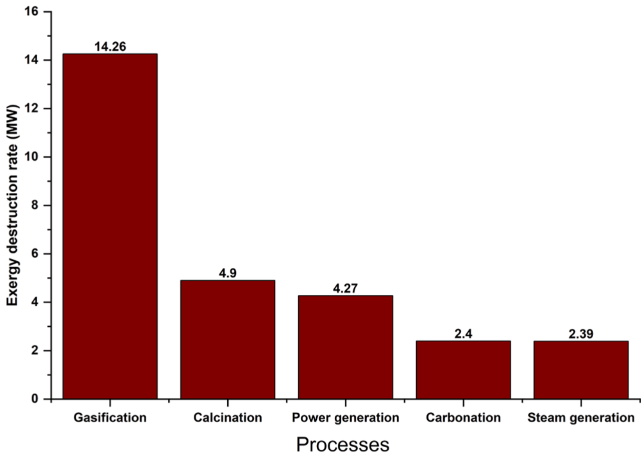

Fig. 11. Exergy destruction rate of each sub-process within the system.

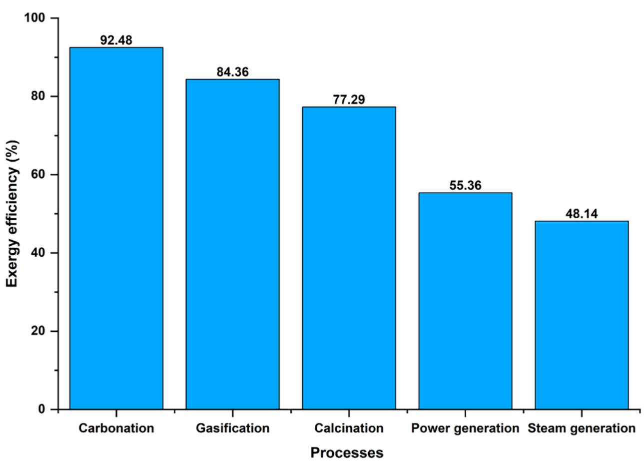

Fig. 12. Exergy efficiency of each sub-process within the system.

calciner and carbonator, causing a decline in exergy efficiency. Moreover, an increase in SB results in reduced exergy losses in the carbonator and gasifier but heightened losses in the calciner reactor, power cycle, and HRSG. The overall rise in exergy loss in the calciner reactor and HRSG surpasses the reduction in the carbonator reactor and gasifier, culminating in a decrease in exergy efficiency as SB increases.

After performing the RSM on the current system using Minitab software, multi-objective optimization has been conducted to explore the optimum point for system performance. In Minitab, each response is converted to a desirability value (d) between 0 and 1, where 1 is desirable and 0 is unacceptable. The overall desirability (D) is then determined accordingly [53]:

$$D = \left((d(r_1))(d(r_2))(d(r_3))\cdots(d(r_n))\right)^{\frac{1}{n}} \quad (27)$$

where n stands for the number of responses.

As shown in Fig. 10, the optimum values for the parameters SB and CE in this study were calculated as 0.5357 and 65 %, respectively. At this point, the optimal energy efficiency, exergy efficiency, and LCOE were determined as 71.89 %, 67.20 %, and 7.88 $/MWh, respectively. The combined desirability for the generated model is approximately 0.9, indicating that the model is deemed acceptable.

4.4. Performance of the system in the optimum condition

The study has determined the optimal point for the three objectives, and this section focuses on investigating and presenting the system's performance at that identified point.

Table 8
Summary of techno-economic analysis results for the proposed system under optimum conditions.

Parameter	Value	Unit
Net power generation in the overall system	5.251	MW
H_2 production rate	0.3852	kg/s
Tail gas production rate	3.21	kg/s
Energy efficiency of the secondary power cycle	36.58	%
Heliostat field efficiency	72.44	%
Heliostat field area	0.105	km^2
Total energy efficiency of the overall system	67.2	%
Total exergy efficiency of the overall system	71.89	%
LCOE	7.87	$/MWh

4.4.1. Thermo-economic analysis

At its optimum condition, the present system produces 5.25 MW electrical power. As co-products, the system generates 0.38 kg/s of H_2 and 3.21 kg/s of tail gas, both with a significant heating value. This results in an impressive 67.2 % energy efficiency.

The input exergy of the system is provided by solar radiation and the chemical exergy of MSW and makeup flow. Exergy analysis indicates that around 28.1 % of the input exergy is destructed in the overall system. The carbonator and gasifier function under steady-state conditions with exergy efficiencies of 92.48 % and 84.6 %, leading to the destruction of 2.4 MW and 14.26 MW of the input exergy, respectively. The calciner reactor operates transitory in accordance with solar radiation, leading to a varying exergy destruction rate throughout the year. However, the yearly mean exergy destruction rate for the calciner reactor is computed at 4.9 MW, achieving a 77.29 % exergy efficiency. Figs. 11 and 12 illustrate the exergy destruction rate and exergy efficiency of the primary sub-processes within the proposed system, respectively.

The gasification process demonstrates the highest exergy destruction rate compared to other processes. According to Fig. 12, the gasification process has the highest exergy efficiency following the carbonation process. The heightened destruction rate of the gasification process can be attributed to substantial exergy flows in the inlet and outlet. The carbonator reactor significantly contributes to boosting the overall system efficiency, thanks to its superior exergy performance and minimal destruction of available energy. In contrast, the steam generation process, which includes the evaporation subprocess and exhibits phase change characteristics, displays the lowest exergy efficiency and dissipates the majority of its input exergy.

The integrated system in this study, considering all co-products shows an LCOE of 7.87$/MWh. For a completely renewable energy-fueled system with the CO_2 capture process and significant investments in CaL reactors and the heliostat field, it sounds promising. Table 8 summarizes the overall system performance from the techno-economic point of view under optimum conditions.

4.4.2. Emergy analysis

According to the energy balance and emergy analysis, the emergy input flows and the emergy indices have been calculated and are presented in Table 9.

According to the emergy analysis results, the proposed system, with only 0.22 of the %R, has low dependency on non-renewable sources. This is attributed to feeding the system with renewable energy sources. The EYR index is calculated to be about 6.62, indicating that the proposed system is not highly dependent on economic inputs; its effect on the ELR is also evident, with no significant environmental impacts. Furthermore, the ESI index confirms that the proposed system is not unsustainable and exhibits a considerable level of sustainability (medium-term sustainability).

Compared to the developed systems in the references [15,48], which are co-generation energy systems, the system presented in this study exhibits better performance in terms of dependency on economic inputs and non-renewable energy sources. The sustainability range in the

Table 9
Emergy input flows and indices for the proposed system under optimum conditions.

Input emergy	Emergy type	Value	Unit	UEV (Sej/unit)	Emergy (Sej/year)
MSW	R	126,144,000	kg/year	99,600,000,000 [15]	1.2564E + 19
Air	R	0	kg/year	51,600,000,000 [15]	0
Solar radiation	R	1,035,642,240	MJ/year	1,000,000 [54]	1.0356E + 15
water	R	88,300,800	kg/year	44,200,000 [15]	3.903E + 15
$CaCO_3$	N	34365409.92	kg/year	1E + 12 [10]	3.4365E + 19
Cost	F	5877817.562	$/year	1.42E + 12	8.3465E + 18
Emergy indices					
%R	EYR	ELR	ESI	EIR	
0.22	6.62	3.4	1.95	0.18	

mentioned study is in the same range as this study. However, comparing different types of systems is not accurate due to their different goals. Nevertheless, since all of them have power generation as one of the co-products, it can provide better insight into the sustainability and environmental factors of the proposed system.

5. Conclusions

This study aims to investigate and optimize a renewable energy-based co-generation system, incorporating a SEG system integrated with a waste heat recovery cycle. In this context, comprehensive analyses, including energy, exergy, economic, and emergy assessments, have been conducted for the entire system. The RSM has been employed to optimize the system's performance with a focus on enhancing energy efficiency, exergy efficiency, and lowering the LCOE. After identifying the optimal point, an in-depth examination was conducted on the effectiveness of the current setup from both technological and economic standpoints under these ideal conditions. Sensitivity analyses were performed across the entire system to evaluate the impact of SB and CE on energy and exergy efficiencies, as well as the LCOE. The results of the parametric study are employed in RSM to optimize system performance, leading to the identification of the optimum point with an SB of 0.53 and CE of 65 %. The optimum energy efficiency of the overall system is determined to be 67.2 % with a net electrical power generation of 5.251 MW. From the second law of thermodynamics perspective, the system exhibits favorable performance with an exergy efficiency of 71.89 % at the optimum point. In terms of cost, this operation condition yields an LCOE of 7.87 $/MWh. Utilizing green energy sources in this system, sustainability analysis indicates that the overall system, with a renewability index of 0.22, demonstrates significant independence from non-renewable inputs. Additionally, with a sustainability index of 1.95, it is considered a medium-term sustainable system. In comparison to conventional co-generation systems (non-renewable energy-based), it outperforms and shows compatibility with other renewable-based co-generation systems, offering a low LCOE.

CRediT authorship contribution statement

Soheil Khosravi: Writing – original draft, Software, Methodology, Investigation, Data curation, Conceptualization. **Dibyendu Roy:** Writing – review & editing, Software, Methodology, Investigation, Data curation. **Rahim Khoshbakhti Saray:** Writing – review & editing, Supervision, Methodology, Conceptualization. **Elaheh Neshat:** Writing – review & editing, Supervision, Methodology, Conceptualization. **Ahmad Arabkoohsar:** Writing – review & editing, Supervision, Methodology, Conceptualization.

Declaration of competing interest

The authors declare that they have no known competing financial interests or personal relationships that could have appeared to influence the work reported in this paper.

Data availability

Data will be made available on request.

References

[1] Leggett LMW, Ball DA. The implication for climate change and peak fossil fuel of the continuation of the current trend in wind and solar energy production. Energy Policy 2012;41. https://doi.org/10.1016/j.enpol.2011.11.022.

[2] Aghaziarati Z, Aghdam AH. Thermoeconomic analysis of a novel combined cooling, heating and power system based on solar organic rankine cycle and cascade refrigeration cycle. Renew Energy 2021;164:1267–83. https://doi.org/10.1016/J.RENENE.2020.10.106.

[3] Khosravi S, Hossainpour S, Farajollahi H, Abolzadeh N. Integration of a coal fired power plant with calcium looping CO2 capture and concentrated solar power generation: energy, exergy and economic analysis. Energy 2022;240:122466. https://doi.org/10.1016/J.ENERGY.2021.122466.

[4] Change IC. Mitigation of climate change. Contribution of Working Group III to the Fifth Assessment Report of the Intergovernmental Panel on Climate Change 2014; 1454:147.

[5] Santos MPS, Hanak DP. Techno-economic feasibility assessment of sorption enhanced gasification of municipal solid waste for hydrogen production. Int J Hydrogen Energy 2022;47:6586–604. https://doi.org/10.1016/J.IJHYDENE.2021.12.037.

[6] Dziva G, Cheng Q, Liu K, Zeng L. Hydrogen production through two-stage sorption-enhanced biomass gasification: process design and thermodynamic analysis. Int J Hydrogen Energy 2023. https://doi.org/10.1016/J.IJHYDENE.2023.06.216.

[7] Dziva G, Jia Z, Xue Y, Zeng L. Hydrogen production from biomass via moving bed sorption-enhanced reforming: kinetic modeling and process simulation. Fuel 2023; 352:129024. https://doi.org/10.1016/J.FUEL.2023.129024.

[8] Osat M, Shojaati F, Osat M. Techno-economic assessment of butanol and pentanol productions from sorption enhanced chemical looping gasification of a lignocellulosic biomass. Renew Energy 2023;217:119176. https://doi.org/10.1016/j.renene.2023.119176.

[9] Zhang C, Li Y, Chu Z, Fang Y. Thermodynamic analysis of integrated sorption-enhanced staged-gasification of biomass and in-situ CO2 utilization by methane reforming process based on calcium looping. Energy Convers Manag 2023;278: 116710. https://doi.org/10.1016/J.ENCONMAN.2023.116710.

[10] Odum HT. Environmental accounting: emergy and environmental decision making. (No Title) 1996.

[11] Brown MT, Ulgiati S. Emergy evaluations and environmental loading of electricity production systems. J Clean Prod 2002;10:321–34. https://doi.org/10.1016/S0959-6526(01)00043-9.

[12] Zhang H, Guan X, Ding Y, Liu C. Emergy analysis of organic rankine cycle (ORC) for waste heat power generation. J Clean Prod 2018;183:1207–15. https://doi.org/10.1016/J.JCLEPRO.2018.02.170.

[13] Paoli C, Vassallo P, Fabiano M. Solar power: an approach to transformity evaluation. Ecol Eng 2008;34:191–206. https://doi.org/10.1016/J.ECOLENG.2008.08.005.

[14] Yazdani S, Salimipour E, Moghaddam MS. A comparison between a natural gas power plant and a municipal solid waste incineration power plant based on an emergy analysis. J Clean Prod 2020;274:123158. https://doi.org/10.1016/J.JCLEPRO.2020.123158.

[15] Jalili M, Chitsaz A, Ghazanfari HS. Sustainability improvement in combined electricity and freshwater generation systems via biomass: a comparative emergy analysis and multi-objective optimization. Int J Hydrogen Energy 2022;47: 2885–99. https://doi.org/10.1016/j.ijhydene.2021.10.245.

[16] Zaman SA, Roy D, Ghosh S. Process modeling and optimization for biomass steam-gasification employing response surface methodology. Biomass Bioenergy 2020; 143:105847. https://doi.org/10.1016/J.BIOMBIOE.2020.105847.

[17] Sharma P, Le MP, Chhillar A, Said Z, Deepanraj B, Cao DN, et al. Using response surface methodology approach for optimizing performance and emission parameters of diesel engine powered with ternary blend of solketal-biodiesel-diesel. Sustainable Energy Technol Assess 2022;52:102343. https://doi.org/10.1016/J.SETA.2022.102343.

[18] Madas SR, Narayanan R, Gudimetla P. Single and multi-objective optimization of PVT performance using response surface methodology with CuO nanofluid

application. Sol Energy 2023;263:111952. https://doi.org/10.1016/J.SOLENER.2023.111952.

[19] Noroozian M, Ghaemi A, Heidari Z. Potential of artificial intelligence and response surface methodology to predict CO2 capture by KOH-modified activated alumina. Case Studies in Chemical and Environmental Engineering 2023;8:100442. https://doi.org/10.1016/J.CSCEE.2023.100442.

[20] Mojaver P, Khalilarya S, Chitsaz A. Multi-objective optimization using response surface methodology and exergy analysis of a novel integrated biomass gasification, solid oxide fuel cell and high-temperature sodium heat pipe system. Appl Therm Eng 2019;156:627–39. https://doi.org/10.1016/J.APPLTHERMALENG.2019.04.104.

[21] Roy D, Samanta S, Roy S, Smallbone A, Roskilly AP. Multi-objective optimisation of a power generation system integrating solid oxide fuel cell and recuperated supercritical carbon dioxide cycle. Energy 2023;281:128158. https://doi.org/10.1016/J.ENERGY.2023.128158.

[22] Sun W, Feng L, Abed AM, Sharma A, Arsalanloo A. Thermoeconomic assessment of a renewable hybrid RO/PEM electrolyzer integrated with Kalina cycle and solar dryer unit using response surface methodology (RSM). Energy 2022;260:124947. https://doi.org/10.1016/J.ENERGY.2022.124947.

[23] Pourali M, Esfahani JA. Performance analysis of a micro-scale integrated hydrogen production system by analytical approach, machine learning, and response surface methodology. Energy 2022;255:124553. https://doi.org/10.1016/J.ENERGY.2022.124553.

[24] Mojaver P, Khalilarya S, Chitsaz A, Jafarmadar S. Performance assessment and optimization of gasification of indigenous biomasses of West Azerbaijan province to attain a hydrogen-rich syngas based on thermodynamic modeling. Biomass Convers Biorefin 2022. https://doi.org/10.1007/s13399-022-03676-7.

[25] Kheiri R, Khoshbakhti Saray R, Omidi KB. Thermo-economic-environmental analysis of a new tri-generation seasonal system with gas turbine prime mover based on municipal solid waste gasification. Energy Convers Manag 2022;265:115755. https://doi.org/10.1016/J.ENCONMAN.2022.115755.

[26] Khalilarya S, Chitsaz A, Mojaver P. Optimization of a combined heat and power system based gasification of municipal solid waste of Urmia University student dormitories via ANOVA and taguchi approaches. Int J Hydrogen Energy 2021;46:1815–27. https://doi.org/10.1016/J.IJHYDENE.2020.10.020.

[27] Khosravi S, Khoshbakhti Saray R, Neshat E, Arabkoohsar A. Towards an environmentally friendly power and hydrogen co-generation system: integration of solar-based sorption enhanced gasification with in-situ CO2 capture and liquefaction process. Chemosphere 2023;343:140226. https://doi.org/10.1016/J.CHEMOSPHERE.2023.140226.

[28] Duan L, Feng T, Jia S, Yu X. Study on the performance of coal-fired power plant integrated with ca-looping CO2 capture system with recarbonation process. Energy 2016;115:942–53. https://doi.org/10.1016/j.energy.2016.09.077.

[29] Michalski S, Hanak DP, Manovic V. Techno-economic feasibility assessment of calcium looping combustion using commercial technology appraisal tools. J Clean Prod 2019;219:540–51. https://doi.org/10.1016/j.jclepro.2019.02.049.

[30] Michael JWagner. Simulation and predictive performance modeling of utility-scale central receiver system power plants. University of Wisconsin-Madison; 2008. MSc Thesis.

[31] Khosravi S, Neshat E, Saray RK. Thermodynamic analysis of a sorption-enhanced gasification process of municipal solid waste, integrated with concentrated solar power and thermal energy storage systems for co-generation of power and hydrogen. Renew Energy 2023;214:140–53. https://doi.org/10.1016/J.RENENE.2023.06.003.

[32] Abanades JC, Anthony EJ, Wang J, Oakey JE. Fluidized bed combustion systems integrating CO2 capture with CaO. Environ Sci Tech 2005;39:2861–6. https://doi.org/10.1021/es0496221.

[33] Siddiqui O, Dincer I. Examination of a new solar-based integrated system for desalination, electricity generation and hydrogen production. Sol Energy 2018;163:224–34. https://doi.org/10.1016/J.SOLENER.2018.01.077.

[34] Khaljani M, Khoshbakhti Saray R, Bahlouli K. Comprehensive analysis of energy, exergy and exergo-economic of cogeneration of heat and power in a combined gas turbine and organic rankine cycle. Energy Convers Manag 2015;97:154–65. https://doi.org/10.1016/J.ENCONMAN.2015.02.067.

[35] Azizi S, Nedaei N, Yari M. Proposal and evaluation of a solar-based polygeneration system: development, exergoeconomic analysis, and multi-objective optimization. Int J Energy Res 2022;46:13627–56. https://doi.org/10.1002/er.8084.

[36] Rahbari HR, Mandø M, Arabkoohsar A. A review study of various high-temperature thermodynamic cycles for multigeneration applications. Sustainable Energy Technol Assess 2023;57:103286. https://doi.org/10.1016/J.SETA.2023.103286.

[37] Nabat MH, Sharifi S, Razmi AR. Thermodynamic and economic analyses of a novel liquid air energy storage (LAES) coupled with thermoelectric generator and Kalina cycle. J Energy Storage 2022;45:103711. https://doi.org/10.1016/J.EST.2021.103711.

[38] Kalan AS, Ghiasirad H, Saray RK, Mirmasoumi S. Thermo-economic evaluation and multi-objective optimization of a waste heat driven combined cooling and power system based on a modified Kalina cycle. Energy Convers Manag 2021;247:114723. https://doi.org/10.1016/J.ENCONMAN.2021.114723.

[39] Farhang B, Ghaebi H, Javani N. Techno-economic modeling of a novel poly-generation system based on biogas for power, hydrogen, freshwater, and ammonia production. J Clean Prod 2023;417:137907. https://doi.org/10.1016/J.JCLEPRO.2023.137907.

[40] Kazmi B, Ali Ammar Taqvi S, Raza F, Haider J, Naqvi SR, Khan MS, et al. Exergy, advance exergy, and exergo-environmental based assessment of alkanol amine- and piperazine-based solvents for natural gas purification. Chemosphere 2022;307:136001. https://doi.org/https://doi.org/10.1016/j.chemosphere.2022.136001.

[41] Jannatabadi M, Farzaneh-Gord M, Rahbari HR, Nersi A. Energy and exergy analysis of reciprocating natural gas expansion engine based on valve configurations. Energy 2018;158:986–1000. https://doi.org/10.1016/J.ENERGY.2018.06.103.

[42] Nakyai T, Authayanun S, Patcharavorachot Y, Arpornwichanop A, Assabumrungrat S, Saebea D. Exergoeconomics of hydrogen production from biomass air-steam gasification with methane co-feeding. Energy Convers Manag 2017;140:228–39. https://doi.org/10.1016/J.ENCONMAN.2017.03.002.

[43] Samimi F, Marzoughi T, Rahimpour MR. Energy and exergy analysis and optimization of biomass gasification process for hydrogen production (based on air, steam and air/steam gasifying agents). Int J Hydrogen Energy 2020;45:33185–97. https://doi.org/10.1016/J.IJHYDENE.2020.09.131.

[44] Bashiri Mousavi S, Nabat MH, Razmi AR, Ahmadi P. A comprehensive study and multi-criteria optimization of a novel sub-critical liquid air energy storage (SC-LAES). Energy Convers Manag 2022;258:115549. https://doi.org/10.1016/J.ENCONMAN.2022.115549.

[45] Bejan A, Tsatsaronis G, Moran MJ. Thermal design and optimization. John Wiley & Sons; 1995.

[46] Rubin ES, Short C, Booras G, Davison J, Ekstrom C, Matuszewski M, et al. A proposed methodology for CO2 capture and storage cost estimates. Int J Greenhouse Gas Control 2013;17:488–503. https://doi.org/10.1016/J.IJGGC.2013.06.004.

[47] Zoelle A, Kuehn N. Quality guidelines for energy system studies. Capital Cost Scaling Methodology: Revision 4 Report 2019.

[48] Deymi-Dashtebayaz M, Norani M. Sustainability assessment and emergy analysis of employing the CCHP system under two different scenarios in a data center. Renew Sustain Energy Rev 2021;150:111511. https://doi.org/10.1016/j.rser.2021.111511.

[49] Qian J, Wu J, Yao L, Mahmut S, Zhang Q. Comprehensive performance evaluation of wind-Solar-CCHP system based on emergy analysis and multi-objective decision method. Energy 2021;230:120779. https://doi.org/10.1016/j.energy.2021.120779.

[50] Palanikumar K, Davim JP. Electrical discharge machining: study on machining characteristics of WC/Co composites. Machining and Machine-Tools 2013:135–68. https://doi.org/10.1533/9780857092199.135.

[51] Roy D. Performance evaluation of a novel biomass-based hybrid energy system employing optimisation and multi-criteria decision-making techniques. Sustainable Energy Technol Assess 2020;42:100861. https://doi.org/10.1016/J.SETA.2020.100861.

[52] Fremaux S, Beheshti SM, Ghassemi H, Shahsavan-Markadeh R. An experimental study on hydrogen-rich gas production via steam gasification of biomass in a research-scale fluidized bed. Energy Convers Manag 2015;91:427–32. https://doi.org/10.1016/J.ENCONMAN.2014.12.048.

[53] Ghodsiyeh D, Golshan A, Izman S. Multi-objective process optimization of wire electrical discharge machining based on response surface methodology. J Braz Soc Mech Sci Eng 2014;36:301–13. https://doi.org/10.1007/s40430-013-0079-x.

[54] Xu A, Wang Y, Song T, Xiong Y, Liu Z, Yang S. Emergy evaluation of a solar-powered cascade system for dehumidification, cooling and heating in hot summer and cold winter areas of China. Energy 2023;278:128057. https://doi.org/10.1016/j.energy.2023.128057.